

Low energy laser initiation of single crystals of β -lead azide

J. T. HAGAN, M. M. CHAUDHRI

Physics and Chemistry of Solids, Cavendish Laboratory, Cambridge, UK

Unfocused low energy Q-switched and non-Q-switched ruby laser irradiation of individual single crystals of β -lead azide of size $40\ \mu\text{m} \times 200\ \mu\text{m} \times 10\ \text{mm}$ has been studied using high-speed photography. It was found that the initiation of fast reaction occurs at isolated sites which are probably defects and act as absorption centres in the dielectric which is otherwise transparent to the ruby wavelength of 694.3 nm. It has also been shown that it is the power and not the energy of the incident beam that controls the initiation under these low energy irradiation conditions. Finally, the variation of the time delay to initiation with the incident laser energy suggests a thermal mechanism of initiation.

1. Introduction

The problem of initiation of fast-sustaining reaction (hereafter called initiation) in reactive solids and damage in inert dielectric which are normally transparent to laser radiation is not well understood. Several mechanisms have been proposed to explain the absorption of the laser energy by the material and the ensuing damage. It is generally accepted that the basic absorption processes in most laser-dielectric interactions occur at impurity centres and/or inhomogeneities (e.g. cracks, vacancy clusters, dislocations etc) in the dielectric [1-4]. However, with the focused beams normally employed in these experiments, the energy densities ($\sim 200\ \text{J cm}^{-2}$ for non-Q-switched beam) and powers ($\sim 100\ \text{MW}$ for Q-switched beam) at the focus are so high that several energy absorption processes such as multiphoton absorption [5,6], dielectric breakdown [7], stimulated Brillouin scattering [8,9] and self-focusing [10,11] may also occur simultaneously. Any one of the above processes can lead to high temperatures and pressures which would damage inert dielectrics or cause initiation in reactive solids [12-14].

Very little work has been reported on the initiation of transparent reactive solids by laser beams apart from the studies by Brish *et al.* [15,16], Yang and Menichelli [17] and Volkova *et al.* [18]. Brish *et al.* have investigated the initiation of compacts of pentaerythritol tetranitrate (PETN and

lead azide by focused non-Q- and Q-switched ruby ($\lambda = 694.3\ \text{nm}$) and neodymium glass ($\lambda = 1069\ \text{nm}$) laser beams. They reported that (a) the delay time to detonation, τ , decreased with the increase in the energy density of the beam, (b) the threshold energy density for initiation was constant for large beam diameters, but increased with smaller beam diameters and (c) the required threshold energy density increased with the increasing compaction pressure of the reactive solids. These authors have proposed that initiation occurs by absorption of the incident laser energy in a thin surface layer of the explosive and the subsequent rapid temperature rise generates shock waves which cause initiation [16].

These investigations of the laser initiation of reactive materials were carried out with focused high energy pulsed beams so that very high powers and energy densities were produced at the focus and any one or a combination of the mechanisms listed above could be important. In order to isolate the most likely absorption mechanism, it was decided to examine the effects of low energy unfocused ruby laser Q-switched and non-Q-switched beams of energy densities in the ranges 3 to $30\ \text{mJ cm}^{-2}$ and 4 to $8\ \text{J cm}^{-2}$, respectively, on individual single crystals of β -lead azide in which propagation of reaction occurs very readily [19]; at such low energy densities and powers, processes such as multiphoton absorption, dielectric breakdown,

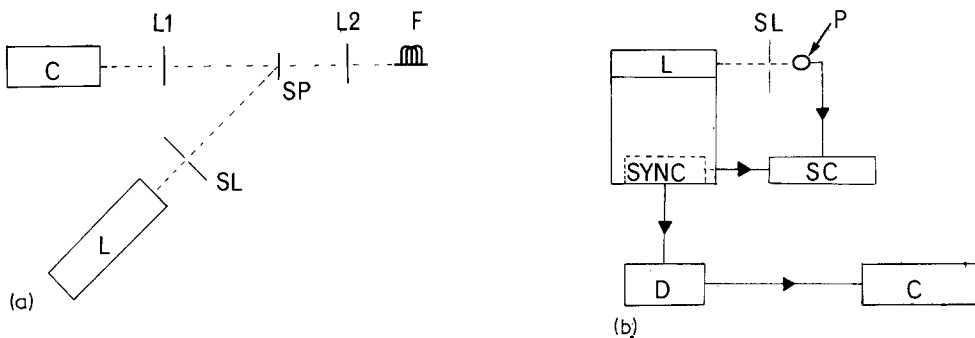


Figure 1 (a) Schematic diagram of the laser and camera arrangement. C and L are camera and laser, respectively, SL is the slit, L1 and L2 are lenses, SP is the lead azide crystal and F is the light source, (b) schematic diagram of the set up for measuring delay time to ignition. P, SC, D and C are the photodiode, oscilloscope, delay unit and camera, respectively, the crystal is between SL and P.

self-focusing and stimulated Brillouin scattering are unlikely.

Lead azide single crystals were chosen for this work because once fast reaction is initiated at even micrometer size "hot spots" in these crystals, rapid propagation occurs readily throughout the entire crystals. On the other hand, the propagation of reaction in the high explosives RDX (cyclotrimethylene trinitramine), HMX (cyclotetramethylene tetranitramine) and PETN only occurs after conditions of confinement, compaction density (for compacts) and pressure pulse are satisfied even when the critical hot spot temperature for initiation has been achieved; these conditions introduce extra complications into the initiation studies of high explosives which were excluded in our investigations.

Since the laser pulses are of short duration (~80 nsec to 0.8 msec) and the time delay to initiation of the reactive solids with which they interact is in the range 0.1 to 1 msec, these studies require high speed recording techniques. For the work described in this paper, high speed framing photography at rates of up to 1 million frames per second has been used to follow the initiation in individual single crystals of β -lead azide under ruby laser irradiation and also to study the delay times to initiation. The results indicate that under low energy irradiation with unfocused Q- and non-Q-switched beams, the initiation in these crystals is probably thermal in origin and it occurs by single photon absorption at isolated defect sites in the crystal. Moreover, the initiation appears to be controlled by the power and not the energy density of the incident beam; this is however contrary to the conclusions of Volkova *et al.* [18] for laser initiation of PETN.

2. Experimental procedures

β -lead azide single crystals were grown by a diffusion method [20]. From the batch of crystals obtained, good quality crystals of dimensions $\sim 40 \mu\text{m} \times 200 \mu\text{m} \times 10 \text{mm}$ were selected for this work. The crystal system is monoclinic and X-ray analysis showed that the *c*-axis of the crystals was along the length. A ruby laser ($\lambda = 694.3 \text{ nm}$) model 351 Bradley type which could be operated in non-Q-switched (duration: 1 msec), or Q-switched modes (duration: 80 nsec) using a dye cell was employed. The crystals were irradiated with the unfocused laser beam.

Two high-speed framing cameras, namely a Beckman and Whitley model 189 rotating mirror type and an Imacon image convertor model 600 type, were used for this work. The former was employed mainly to observe the damage and any initiation occurring in the crystal due to laser irradiation, while time delay to initiation after irradiation was determined with the latter. The experimental arrangement is shown schematically in Fig. 1; in Fig. 1 the beam from laser, L, passes through a slit, SL, of dimensions $2 \text{ mm} \times 15 \text{ mm}$, placed at a distance of 150 mm from the laser window and irradiates the sample, SP, which is positioned along the axis of the laser. The slit is oriented such that its length is along the horizontal diameter of the beam and the crystal length is normal to the slit length.

The sample is back-lit with the flash from a xenon-filled F.A. 5 flash tube, L2 is a condenser lens and L1 is an additional objective for the rotating mirror camera C; the optic axes of the camera and the laser beam are inclined to each other at an angle of 45° . In this set up the laser and the flash tube are triggered by synchronous pulses from the camera control unit.

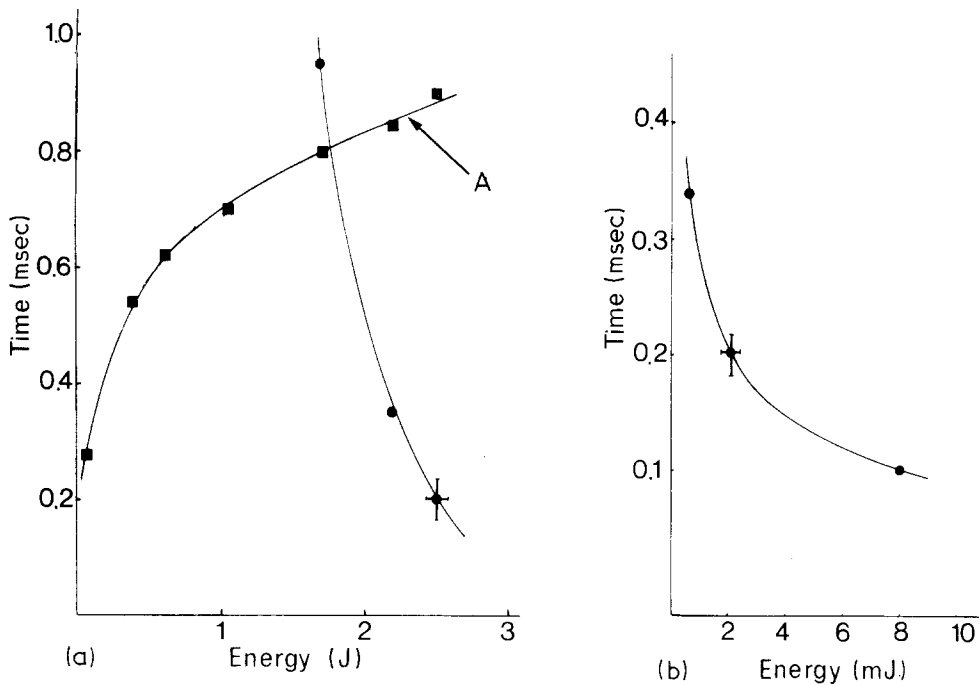


Figure 2 Delay times to ignition as a function of incident energy for (a) non-Q-switched beams and (b) Q-switched beam. The curve, labelled A, is the pulse length at different output energies.

The arrangement for the Imaçon work is illustrated in Fig. 1b. Synchronization of the camera with the event was achieved by taking two synchronous electrical pulses from the "SYNC" output control unit of laser to (i) trigger the trace of an oscilloscope, SC, and (ii) through a delay unit, D, to trigger the Imaçon Camera, C. The signal from a photodiode, P, placed in the path of the beam through the slit, SL, is displayed on the scope trace from which the start of the lasing action is noted. The camera, C, records the moment of initiation in the sample. The time delay between the irradiation of the sample and initiation was obtained from the various quantities, namely, the lasing time, the delay time in the unit, D, and the frame number of the photographic sequence in which the initiation occurs.

The delay time was measured as a function of the beam energy (this was varied by changing the voltage on the discharge lamp) of the laser for both Q- and non-Q-switched modes of operation. The beam energy (the portion transmitted through the slit) was measured with a laser calorimeter (ITL, model 136, 1018) capable of measuring energies in the range 1 mJ to 30 J.

In order to calculate the temperature rise in the β -lead azide we need the value of the absorption coefficient of the crystals at the laser wavelength.

This was obtained by taking an optical absorption spectrum of a good quality crystal using a Perkin Elmer 323 spectrometer.

3. Results

3.1. Threshold energies

First, the threshold energies for the initiation in these crystals for both Q- and non-Q-switched pulses were established as 1.5 mJ cm^{-2} and 4.5 J cm^{-2} , respectively. The value of 4.5 J cm^{-2} is in good agreement with 4.9 J cm^{-2} for non-Q-switched pulses for the case of dextrinated lead azide powder at a loading pressure of 14 MPa [21]. Other workers give data for powders for unfocused [15] and focused [20] beams; our value of 1.5 mJ cm^{-2} for a Q-switched beam is ~ 40 times smaller than the value reported by Brish *et al.* [15, 16]. On the other hand the value given by Field *et al.* [20] is two orders of magnitude higher than our value for non-Q-switched beam. The causes of this are not clear.

3.2. Delay times

The delay times between the irradiation and initiation of the crystals as a function of the incident energy density for both non-Q-switched and Q-switched pulses are shown in Fig. 2a and b; each point on the graphs represents an average of 10

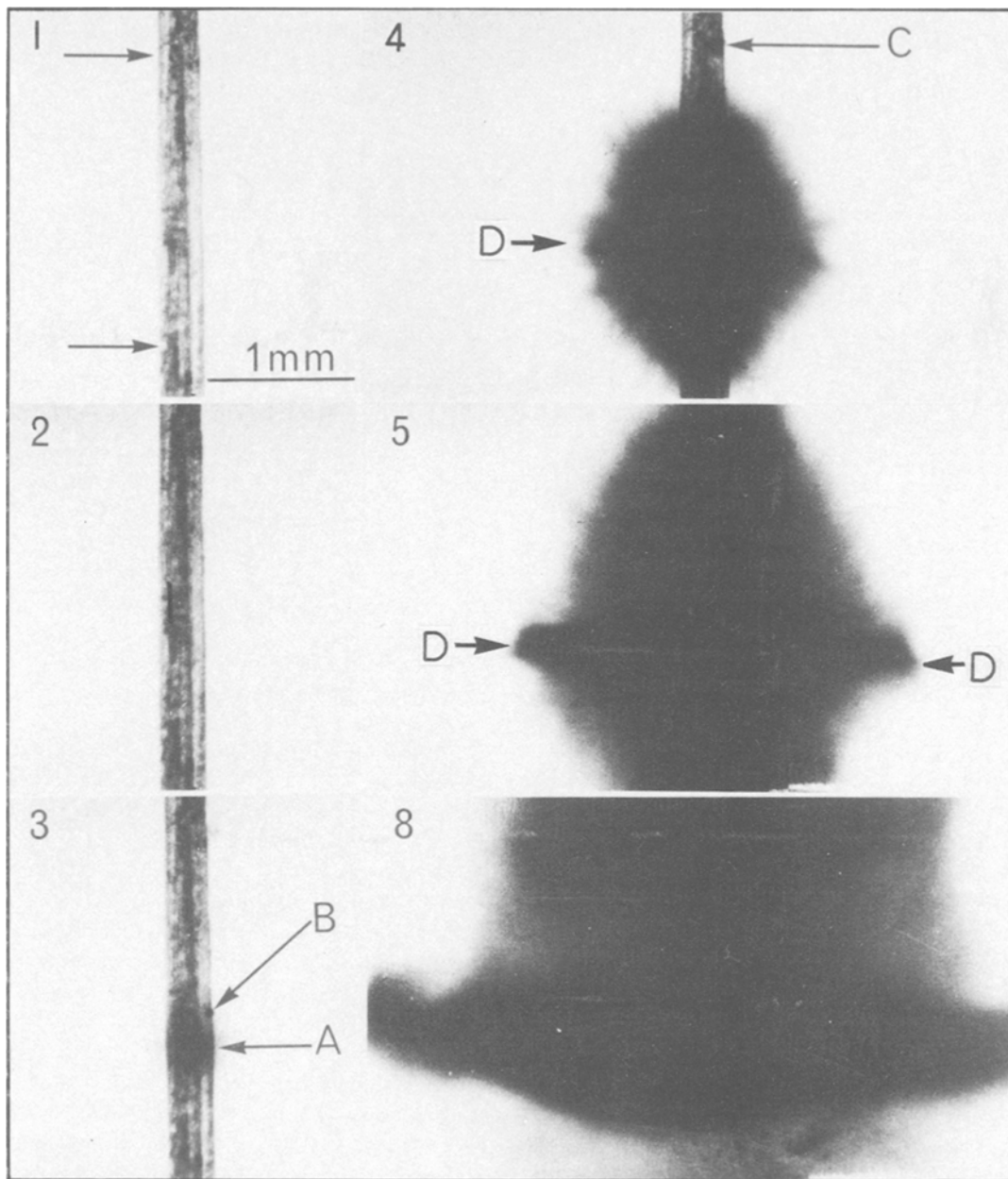


Figure 3 High-speed photographic sequence of laser initiation of β -lead azide taken with the Beckman-Whitley 189 camera at a framing rate of $1\mu\text{sec}$ per frame. The arrows in frame 1 mark the region of the crystal under irradiation. The arrows marked A, B and C in frames 3 and 4 show the initiation sites.

measurements and the representative errors are also shown. It was found that for the non-Q-switched beam the duration of the pulse increased with the output energy (see Graph A in Fig. 2a).

It will be seen from Fig. 2a and b that the energy of the Q-switched beam is considerably smaller than that of the non-Q-switched pulses for a similar time delay to initiation. Moreover, delay time to initiation also decreases inversely with the

beam energy for both types of pulse; such a dependence has been attributed to a thermal mechanism of initiation [16].

3.3. High-speed photographic sequences

High-speed framing photography revealed a number of interesting features of the initiation and propagation of reaction. Initiation, especially with the non-Q-switched beam, always occurred at dis-

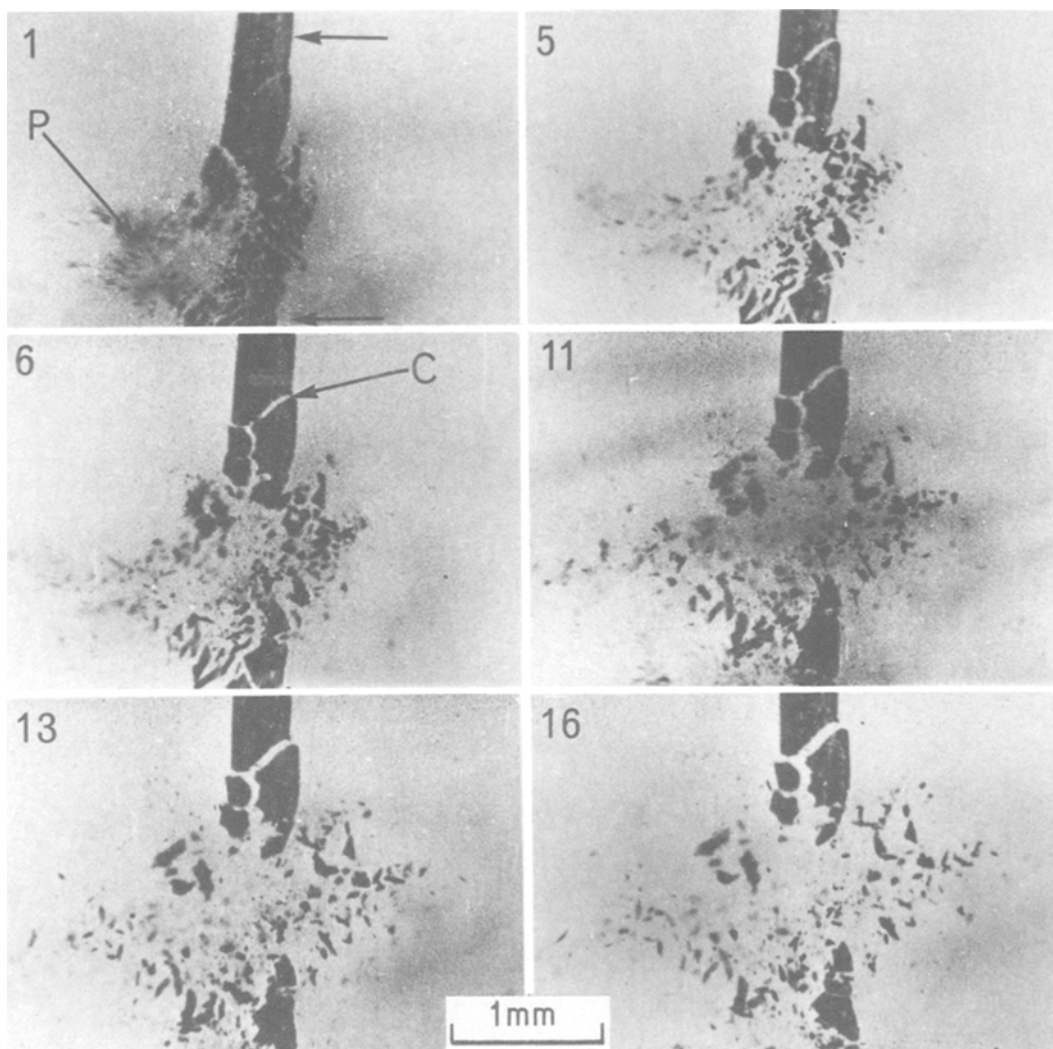


Figure 4 High-speed sequence of non-Q-switched laser initiation of β -lead azide crystal. Framing rate is $1 \mu\text{sec}$ per frame. The sequence shows initiation and fragmentation of the crystal. Again the arrows in frame 1 show the region of crystal under irradiation.

crete localized sites. Occasionally, for incident beam energy densities near the initiation threshold value, violent fragmentation of the crystal also took place. A typical high-speed camera sequence, taken at $1 \mu\text{sec}$ per frame of the initiation with a non-Q-switched pulse is shown in Fig. 3. The energy density of the beam was 5 J cm^{-2} , which is just above the threshold value of 4.5 J cm^{-2} . The arrows in frame 1 mark the region of the crystal irradiated (the total irradiation time was $\sim 800 \mu\text{sec}$). Initiation occurs at regions A and B as indicated by the formulation of the gaseous reaction products. The reaction spreads along the length of the crystal at a speed of $\sim 730 \text{ msec}^{-1}$, which is in agreement with earlier work [20]; one

microsecond later (i.e. frame 4) another initiation site is formed at C. Frames 5 and 8 show the expansion of the gaseous reaction products. Note that the reaction cloud has bulged out at the point where initiation took place first (see point D).

Another sequence, taken at $4 \mu\text{sec}$ per frame, of the fragmentation of a crystal by a non-Q-switched beam of energy density 5 J cm^{-2} is shown in Fig. 4. In frame 1 the irradiation has occurred for $\sim 950 \mu\text{sec}$, and the crystal has broken into several fragments. Judging by the distance to which the fragments have scattered and the expanse of the dark reaction products, it can be said that the reaction was initiated but failed to propagate. The size of the fragments is in the range 10 to $300 \mu\text{m}$

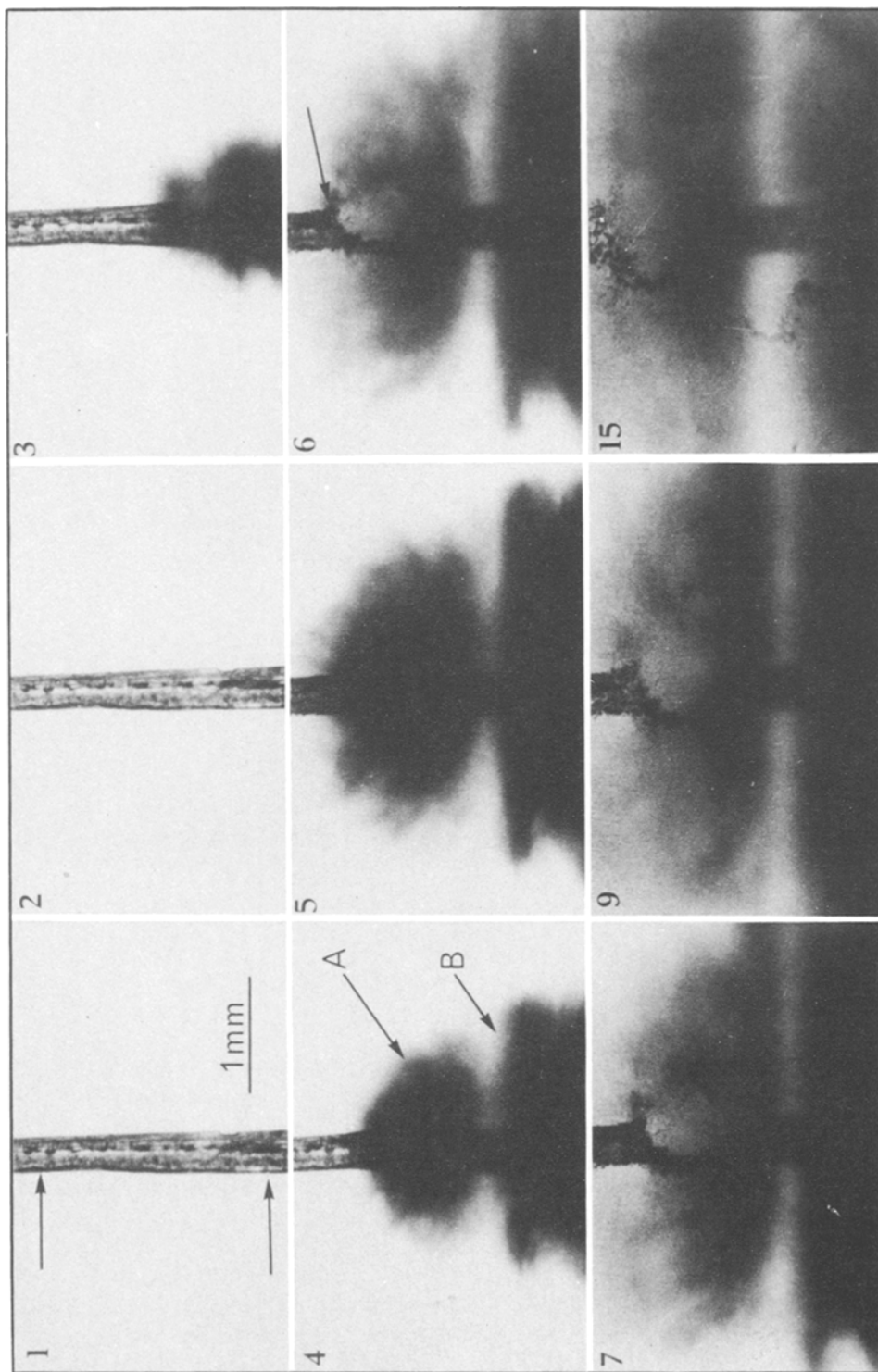


Figure 5 Beckman-Whitley high-speed photographic sequence at 1 μ sec per frame of non-Q-switched laser initiation. The regions under irradiation are marked in frame 1. The initiation has taken place at two places A and B in frame 4 but it ceases in frame 6 because of cracking.

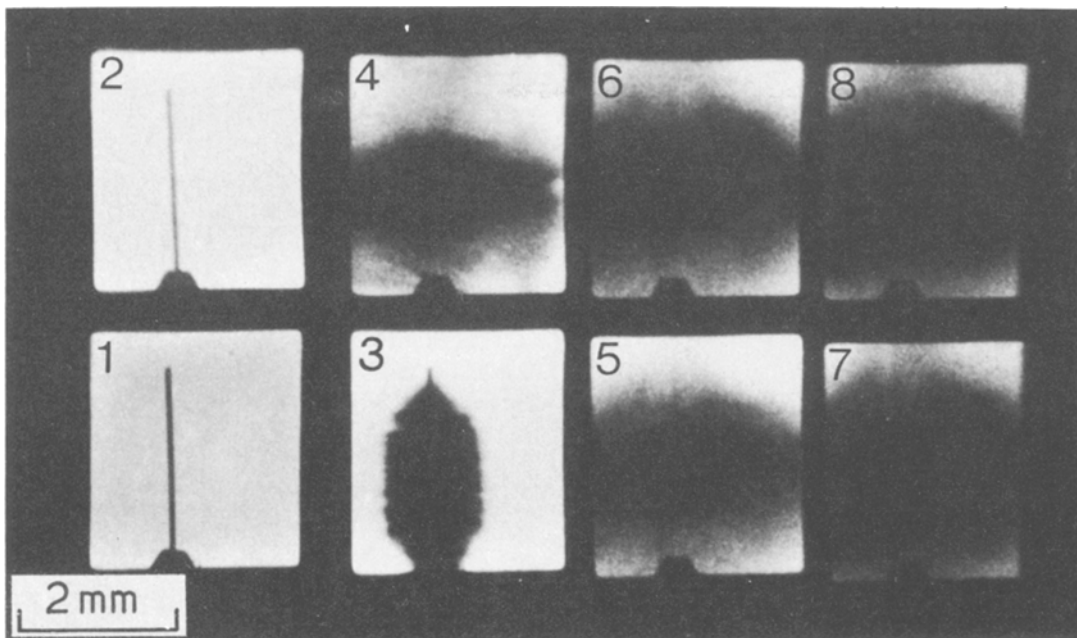


Figure 6 Imacon high-speed sequence of Q-switched laser irradiation of β -lead azide crystal. The framing rate is $4 \mu\text{sec}$ per frame. It shows the corrugated and serrated barrel nature of the decomposition products in frame 3 and it is indicative of simultaneous initiation at different sites on the crystal.

and their velocities are up to 100 msec^{-1} . Clearer evidence for the cracking of the crystal is indicated by C in frame 6; such a crack which cuts right across the width of the crystal would tend to stop the propagation of the reaction. In fact, we have observed that in some cases a propagating reaction stops altogether after having travelled some distance. An example is shown in Fig. 5; the reaction is initiated in frame 3, but ceases completely in frame 6. Similar observations have been reported by Chaudhri and Field [22] for single crystals of β -lead azide in which reaction was initiated by an exploding bridgewire. They have attributed the failure of propagation to the inability of the reaction to continue across large physical discontinuities (such as cracks) in the crystals.

With the Q-switched beam and for energies above the threshold values, the initiation appeared

to occur simultaneously (i.e. in a time much less than the interframe time of 1 to $5 \mu\text{sec}$) over the entire irradiated surface of the crystal. A sequence taken with the Imacon camera is shown in Fig. 6. It is uncertain whether with the Q-switched beam the reaction is also initiated at discrete points. It can, however, be inferred from the corrugated edges of the barrel-shaped reaction products that the reaction may have started simultaneously at several closely spaced localized sites.

3.4. The optical absorption spectrum of the crystals

The absorption spectrum was measured in the wavelength range 340 to 2600 nm, but in Fig. 7 we show the room temperature results for the wavelength region up to 700 nm only for a $24 \mu\text{m}$ thick β -lead azide crystal. It will be seen that the absorp-

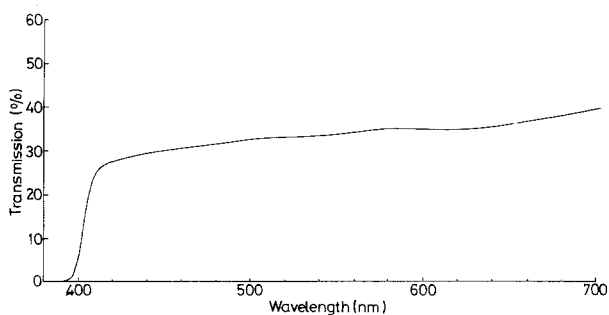


Figure 7 Absorption spectrum of $24 \mu\text{m}$ thick β -lead azide crystal in the wavelength range 340 to 700 nm.

tion edge is in the wavelength region 390 to 420 nm. For longer wavelengths the transmission gradually increases to 40% for the ruby laser wavelength of 694.3 nm. (It should be mentioned that no peaks were observed up to the longest wavelength used i.e. $\lambda = 2600$ nm.) The absorption spectrum of the sample cooled down to the liquid nitrogen temperature was also obtained; no structure appeared in the absorption edge, but the edge shifted slightly to a lower wavelength range of 380 to 400 nm.

An estimate of the reflectivity of the crystal surface may be made from the knowledge of its refractive indices; the values quoted by McCrone [23] in the crystallographic directions a , b and c are 1.98, 2.14 and 2.7, respectively. As in our experiments the beam direction was along the a -axis, we take the average of the refractive indices in the other two directions and estimate the reflectivity as 0.17. By taking into account the reflection from the front surface and ignoring the rear surface, α , the absorption coefficient may be determined from

$$T(1 - R_0^2 e^{-2\alpha d}) = (1 - R_0)^2 e^{-\alpha d} \quad (1)$$

where T is the transmission, R_0 the reflectivity and d , the crystal thickness in the beam direction. The value of α at 694.3 nm is $2.3 \times 10^4 \text{ m}^{-1}$.

4. Discussion

β -lead azide crystals are transparent to the ruby laser wavelength. For $\alpha = 2.3 \times 10^4 \text{ m}^{-1}$ and an incident energy of 1 J cm^{-1} , we estimate a temperature rise of less than 2 K in the crystal. The area of the slit is $3 \times 10^{-5} \text{ m}^2$ so that from Fig. 2, incident energies of 4.5 J cm^{-2} and 1.5 mJ cm^{-2} for the cases of non-Q-switched and Q-switched beams, respectively, cause initiation in these crystals and as non-thermal processes such as cracking and fragmentation are unlikely to be important [24], it needs to be explained how the necessary ignition temperature of at least 680 K is attained.

We now consider the localized nature of the process of initiation of reaction as revealed by high-speed photography (see Fig. 3). These observations indicate that at these isolated regions, the initiation temperature is attained due to the high absorption of the incident beam energy. These absorption centres are probably metallic inclusions which are less than $1 \mu\text{m}$ in size since they are not resolvable under an optical microscope. Such impurities are

known to have a profoundly degrading effect on the laser damage threshold of inert dielectrics [3, 4]. At the very low energy densities used in our experiments, single photon absorption by these impurities is the most likely absorption process for producing sufficiently high localized temperature rises.

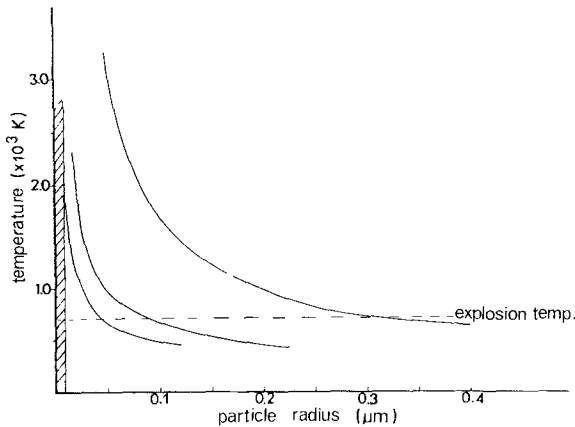
Further support for the thermal mechanism of initiation comes from the time delay, τ , against energy measurements. It has been shown that τ is much shorter for the Q-switched beam than that for the non-Q-switched beam, even though the energy density is much less in the former. An examination of the data shown in Fig. 2a and b indicates that τ is controlled by the power rather than the energy density of the incident beam. As an example, for $\tau = 300 \mu\text{sec}$, the energy densities for the Q-switched (pulse duration 80 msec) and non-Q-switched (duration 850 μsec) pulses are 3 mJ cm^{-2} and 7.2 J cm^{-2} , respectively; the corresponding powers for the two beams are $3.75 \times 10^4 \text{ W}$ and $8.4 \times 10^3 \text{ W}$, respectively. Note, however, that while the energy densities in the two cases are different by 3 orders of magnitude, the power of the beams are approximately the same; this gives an indication of the controlling process. Similar observations have been reported for the initiation of laser damage in inert dielectrics by Arkhipov *et al.* [25]. These authors have also suggested that the most probable cause of the damage is the thermal explosions at defect or impurity centres.

In the lead azide crystals the most likely inhomogeneities are colloidal lead particles. It is possible to estimate the temperature rise of these particles for a given laser pulse. As the thermal conductivity of lead azide is much smaller than that of the lead particles, we assume that these particles are perfectly conducting and are in perfect contact with the crystal matrix and that the particles lose heat by conduction alone.

The solution to such a problem has been given by Carslaw and Jaeger [26], and the average temperature rise, ΔT , of an impurity particle is given by

$$\Delta T \approx \frac{3\epsilon_\lambda J t}{4C_{vi}R_i} K$$

for short-time irradiation or large particles ($R_i \gg (D_g t)^{1/2}$) and



$$\Delta T \approx \frac{\epsilon_{\lambda} J R_i}{4 K_g} \times \left[1 - \frac{R_i}{(\pi D_g t)^{\frac{1}{2}}} - \frac{R_i^3 (2-q)}{2q \pi^{\frac{1}{2}} (D_g t)^{\frac{3}{2}}} \right] \text{K}$$

for long-time irradiation or small particles ($R_i \ll (D_g t)^{1/2}$) where $q = 3C_{vm}/C_{vi}$ and C_{vm} and C_{vi} are the specific heats for the matrix and the inclusion, respectively. J is the radiation flux per unit time, t , the pulse duration, ϵ_{λ} the emissivity and R_i is the radius of the particle. To avoid complicated conduction problems associated with long-time irradiation with the non-Q-switched beam, only Q-switched data will be considered here.

Fig. 8 shows the temperature rise variation with particle size for the Q-switched beam at 3 different energies used in these experiments. The physical constants of β -lead azide are listed in Appendix 1. It will be seen from the curves in Fig. 8 that as the incident energy is increased the size of the particle which attains the initiation temperature also increases. However, since the time delay to initiation is a sensitive function of the "hot spot" temperature as predicted by thermal explosion theories, the controlling size will be the one for which the temperature rise is the maximum. This is supported by our experimental observations that for a given incident energy the time delay to initiation is constant.

From the temperature rise against particle size curve for the Q-switched beam of the threshold energy we can also find the minimum size of the lead particles; for these crystals the radius of this minimum size particle is $0.04 \mu\text{m}$, which is consistent with the fact that under an optical microscope the inclusion particles are not visible.

It should be stated that lead particles of dia-

Figure 8 Shows the variation of temperature with the radius of the absorption impurity for Q-switched beam at three different energies, used in the experiments. Curves a, b and c represent 1, 2 and 8 mJ incident energies, respectively. The explosion temperature of β -lead azide is also indicated.

meter less than 10 nm are unlikely to cause initiation even if their temperatures are ~ 1000 to 2000 K. Evidence in support of this comes from the experiments of Bowden and co-workers [26] who irradiated heavy metal azides with neutrons and fission fragments, in order to produce very small size "hot spots", without causing initiation. Rough calculations show that in these experiments "hot spots" of an approximate diameter of 10 nm and temperature of 2000 K may have been reached within the material.

At present, kinetics of decomposition of β -lead azide at high temperatures, such as attained in these experiments, is not known. It should be possible to calculate the time delay to initiation for different beam energies using the time-dependent thermal theory of explosion and compare these with the measured values using the critical particle size of $0.04 \mu\text{m}$ for all three incident energies.

5. Conclusion

Initiation of individual β -lead azide single crystals by unfocused ruby laser pulses of low energy densities, both Q-switched and non-Q-switched, has been shown to occur at isolated microscopic regions, which are probably lead particles. By measuring the time delay to initiation for different incident energies, it has been argued that the initiation is thermal in origin. Finally, we may conclude that under suitable conditions for propagation of a fast reaction, initiation in secondary explosives containing microscopic inclusion particles may also be achieved by unfocused low energy density laser pulses.

Acknowledgement

This work was supported by the US Army

Armanent Research and Defence and the Ministry of Defence (Procurement Executive).

Appendix 1

Properties of β -lead Azide:

Density, $\rho = 4.9 \times 10^3 \text{ kg m}^{-3}$;

Specific heat, $c = 3.8 \times 10^2 \text{ J kg}^{-1}$;

Heat of reaction, $Q = 1300 \times 10^2 \text{ J kg}^{-1}$;

Activation energy, $E = 168 \times 10^3 \text{ J mol}^{-1}$;

Frequency factor, $Z = 10^{13} \text{ sec}^{-1}$;

Thermal conductivity, $K = 16 \times 10^{-2} \text{ J m}^{-1} \text{ sec}^{-1} \text{ K}^{-1}$.

Appendix 2

Properties of lead:

Emissivity, $\epsilon_\lambda = 0.3$;

Density, $\rho = 11.4 \times 10^3 \text{ kg m}^{-3}$;

Specific heat, $c = 1.38 \times 10^2 \text{ J kg}^{-1} \text{ K}^{-1}$;

Thermal conductivity = $34.6 \text{ J m}^{-1} \text{ sec}^{-1} \text{ K}^{-1}$.

References

1. M. B. AGRANAT, F. N. CHERNAYAVSKY, N. P. NOVILOV, S. S. SALUENYA, P. N. YAMPOLSKY and YU. I. YUDIN, *Nature* **226** (1970) 349.
2. R. W. HOPPER and D. R. UHLMANN, *J. Appl. Phys.* **41** (1970) 41.
3. N. Y. VOLKOVA, *Sov. Phys. Sol. St.* **12** (1970) 1742.
4. *Idem, ibid.* **12** (1970) 470.
5. A. M. BRONCH-BRUEVICH and V. A. KHODOVOI, *Sov. Phys. Uspekhi* **1** (1968) 38.
6. G. I. ASEEV and M. I. KATS, *Sov. Phys. Sol. St.* **14** (1972) 1122.
7. A. A. WASSERMAN, *Appl. Phys. Lett.* **10** (1967) 132.
8. R. J. CHIAO, C. H. TOWNES and B. P. STOICHEFF, *Phys. Rev. Lett.* **12** (1964) 592.
9. G. R. GIULIANO, *Appl. Phys. Lett.* **5** (1964) 137.
10. R. J. CHIAO, E. GARMIRE and C. H. TOWNES, *Phys. Rev. Lett.* **13** (1964) 479.
11. G. M. ZVEREV, T. N. MIKAILOVA, V. A. PASHKOV and N. M. SOLEVEVA, *Sov. Phys. JETP* **5** (1969) 319.
12. D. W. HARPER, *Brit. J. Appl. Phys.* **16** (1965) 751.
13. E. KOCHER, L. TSCHUDI, J. STEFFEN and G. HERZIGER, *IEEE J. Quantum Electronics* **QE8** (1972) 120.
14. C. E. BELL and J. A. LANDT, *Appl. Phys. Lett.* **10** (1967) 46.
15. A. A. BRISH, I. A. GALEEV, E. A. ZAITSEV, E. A. SBITNEV and L. V. TATARINTSEV, *Fiz. Gorenija Vzryva (Trans.)* **2** (1966) 132.
16. *Idem, ibid.* **5** (1967) 475.
17. L. C. YANG and V. MANICHELLI, *Appl. Phys. Lett.* **19** (1971) 473.
18. A. A. VOLKOVA, A. D. ZINCHENKO, I. V. SANIN, V. I. TARZHANOV and B. B. TOKAREV, *Fiz. Gorenija i Vzryva* **13** (1977) 760.
19. M. M. CHAUDHRI, PhD Thesis, Cambridge (1969).
20. J. E. FIELD, P. N. POPE and M. A. ZAFER, "A report on laser initiation of explosives". Cavendish Lab. Cambridge, April 1979.
21. Jet Propulsion Laboratory Technical Report, 32-1474, "A study of the sensitivity of pyrotechnic materials to laser energy" (1969).
22. M. M. CHAUDHRI and J. E. FIELD, 5th International Symposium on Detonation, Pasadena, Calif., USA (Office Naval Research ACR-184, Washington DC, 1970) p. 301.
23. W. C. McCURONE, US Clearing House, Red. Sci. Techn. Information, 659793 (1963).
24. M. M. CHAUDHRI, *Combustion and Flame* **19** (1972) 419.
25. YU. V. ARKHIPOV, N. V. MORACHEVSKII, V. V. MOROZOY, F. S. FAIZULLOV, *Sov. Phys. Sol. St.* **14** (1972) 1510.
26. H. S. CARSLAW and J. C. JAEGER, "Conduction of Heat in Solids", 2nd edn. (Oxford University Press, London, 1959).
27. F. P. BOWDEN, 9th International Symposium on Combustion, 1963 (Academic Press, New York, 1963).

Received 16 January and accepted 26 February 1981.